Electronic Supplementary Material (ESI) for Nanoscale.

Electronic Supplementary Information

Continuous syntheses of Pd@Pt and Cu@Ag core–shell nanoparticles using microwave-assisted core particle formation coupled with galvanic metal displacement

Masato Miyakawa,*[a] Norihito Hiyoshi,[a] Masateru Nishioka,*[a]
Hidekazu Koda,[b] Koichi Sato,[a] Akira Miyazawa,[a]
and Toshishige M. Suzuki[a]

[a]*National Institute of Advanced Industrial Science and Technology, AIST,*
4-2-1, Nigatake, Miyagino-ku, Sendai, 983-8551, Japan
[b]*Shinko-Kagaku Co. Ltd.*
1544-19, Mashimori, Koshigaya-shi, Saitama, 343-0012, Japan

E-mail: masato-miyakawa@aist.go.jp, m-nishioka@aist.go.jp

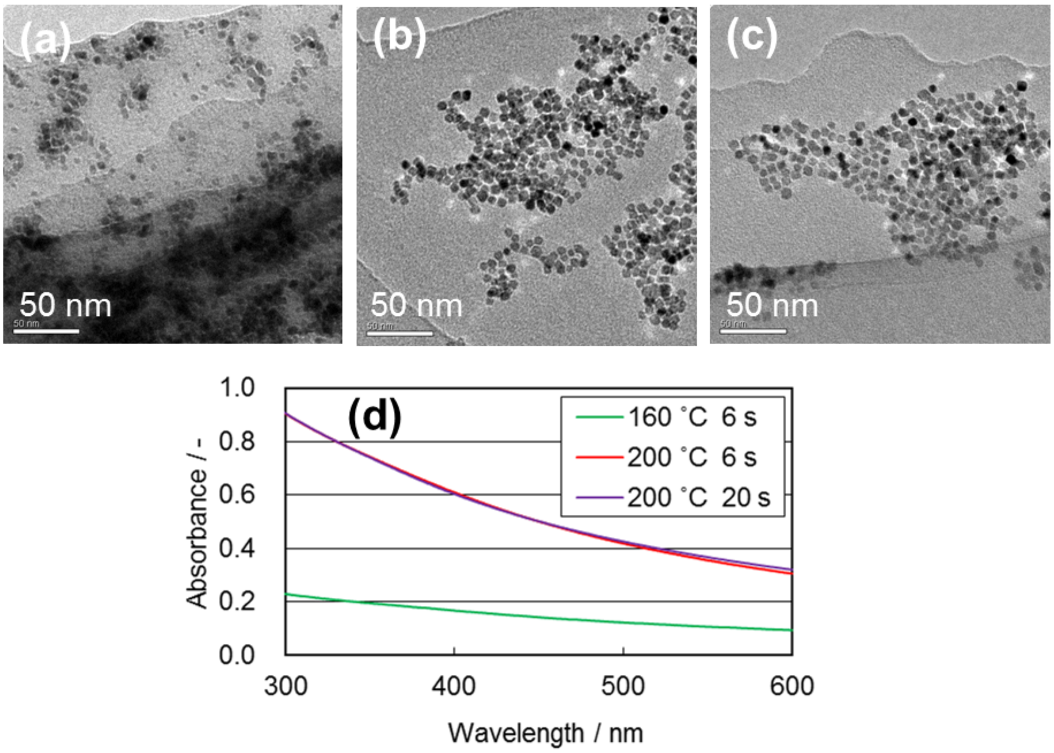

Fig. S1 (a–c) TEM images of Pd nanoparticles synthesized using the MW flow reactor: (a) 160 °C, reaction time 6 s; (b) 200 °C, reaction time 6 s; and (c) 200 °C, reaction time 20 s. The respective particle sizes were (a) 5.2 ± 1.2 nm, (b) 6.5 ± 0.6 nm, and (c) 6.5 ± 0.6 nm. (d) UV-vis spectra of Pd nanoparticle dispersions. Spectra of 200 °C 6 s and 200°C 20 s were overlapped, suggesting that the reaction was nearly completed within 6 s at 200 °C.

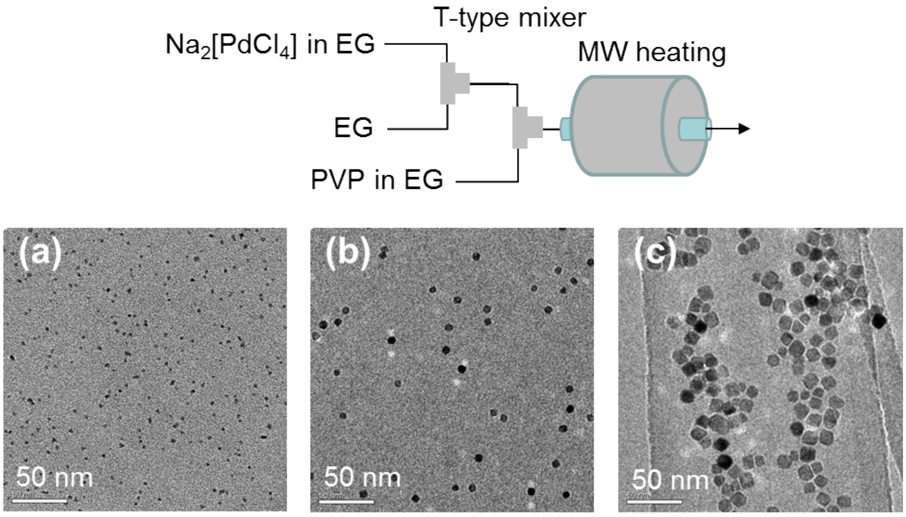

Sample	Na$_2$[PdCl$_4$] / mM	PVP / wt%	Particle size / nm
(a)	10	10	3.1 ± 0.4
(b)	100	15	6.5 ± 0.6
(c)	100	10	11.3 ± 1.4

Fig. S2 TEM images of size-controlled Pd nanoparticles synthesized by varying the concentration of Na$_2$[PdCl$_4$] and PVP using the MW flow reactor (200 °C, 6 s). Separately prepared EG solutions of Na$_2$[PdCl$_4$] and PVP were mixed immediately before feeding to the MW reactor. The particle sizes were controlled within the range of 3.1 – 11.3 nm.

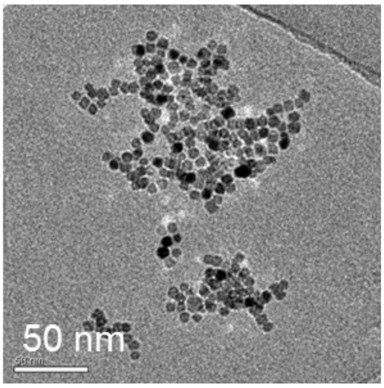

Fig. S3 TEM image of Pd@Pt core–shell nanoparticles. The particle size was estimated as 6.5 ± 0.6 nm, which closely approximates that of the started Pd core nanoparticle.

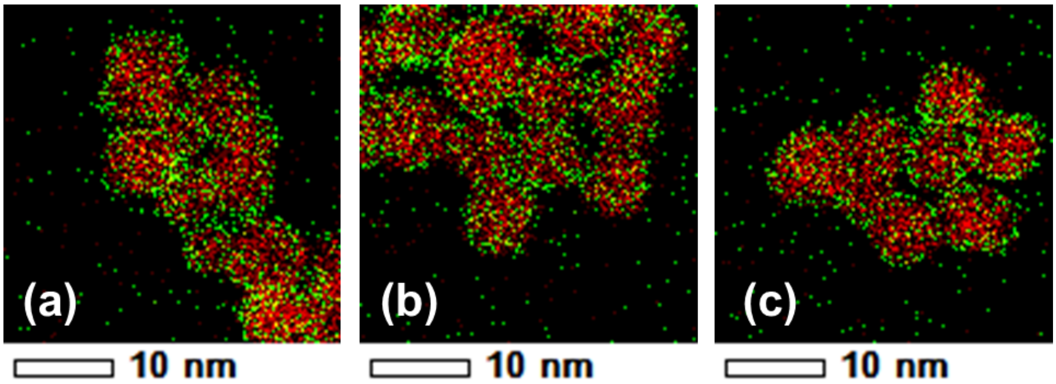

Fig. S4 Time dependence for the grow of Pt shell layer after mixing of Pd nanoparticles with Pt solution and standing for (a) 6 h, (b) 24 h, and (c) 72 h. Pd and Pt are shown as red and green. The EDS atomic ratio was an almost equal value (Pd : Pt = 87 : 13) between 6–72 h.

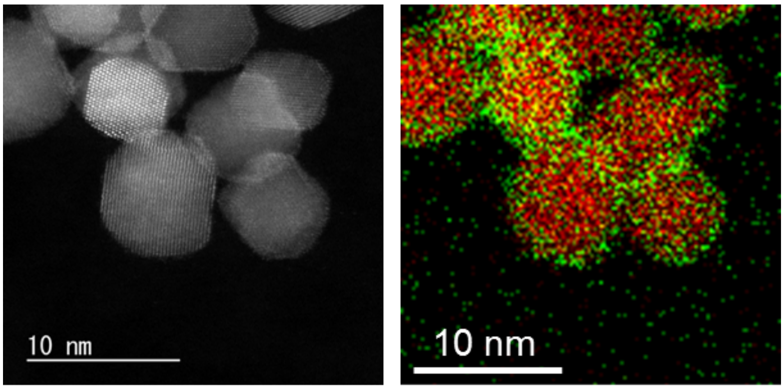

Fig. S5 (a) HAADF-STEM image and (b) elemental mapping image of Pd@Pt core–shell nanoparticles after stored in ethanol for six months. Pd and Pt are shown as red and green colors, respectively. The particle size (6.5 ± 0.6 nm) and the atomic ratio (Pd : Pt = 88 : 12) were similar values with those of as-synthesized sample.

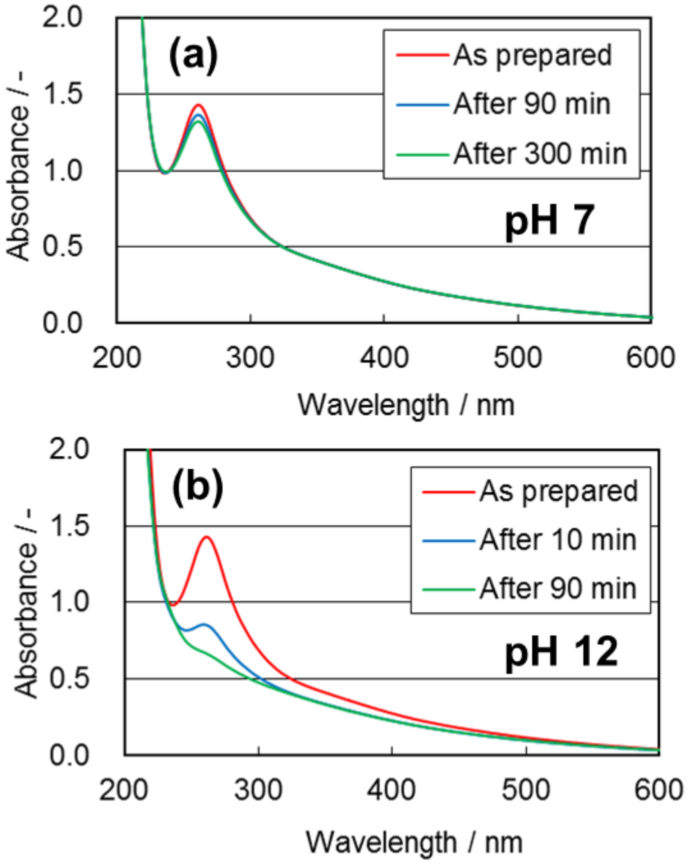

Fig. S6 UV-vis spectral change of the Pd nanoparticle dispersions upon addition of $H_2[PtCl_6]\cdot6H_2O$. (a) pH 7, (b) pH 12. The sharp absorption peak of $[PtCl_6]^{2-}$ at 270 nm gradually disappeared in alkaline condition (pH 12) while change of the peak intensity was very small at pH 7.

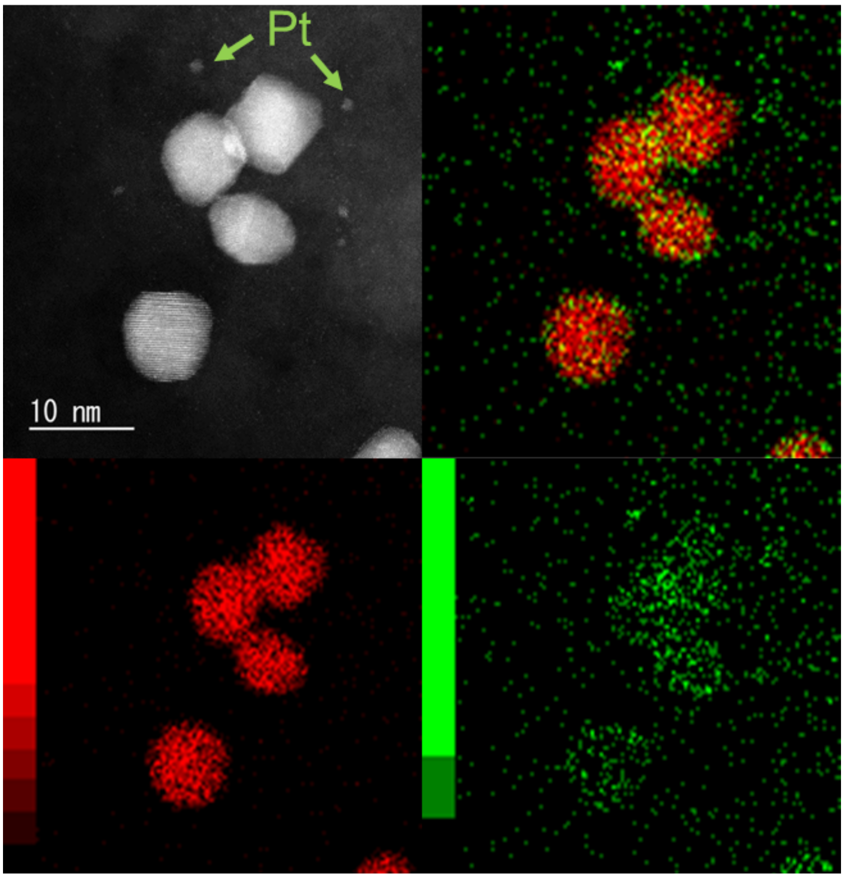

Fig. S7 HAADF-STEM image and elemental mapping image of nanoparticles synthesized at pH 13. Pd and Pt are shown, respectively, as red and green. At extremely high pH (>13), nucleation and growth of single Pt in the bulk solution were enhanced in place of core-shell formation and as the result mixture of Pd@Pt and very fine Pt nanoparticles was formed.

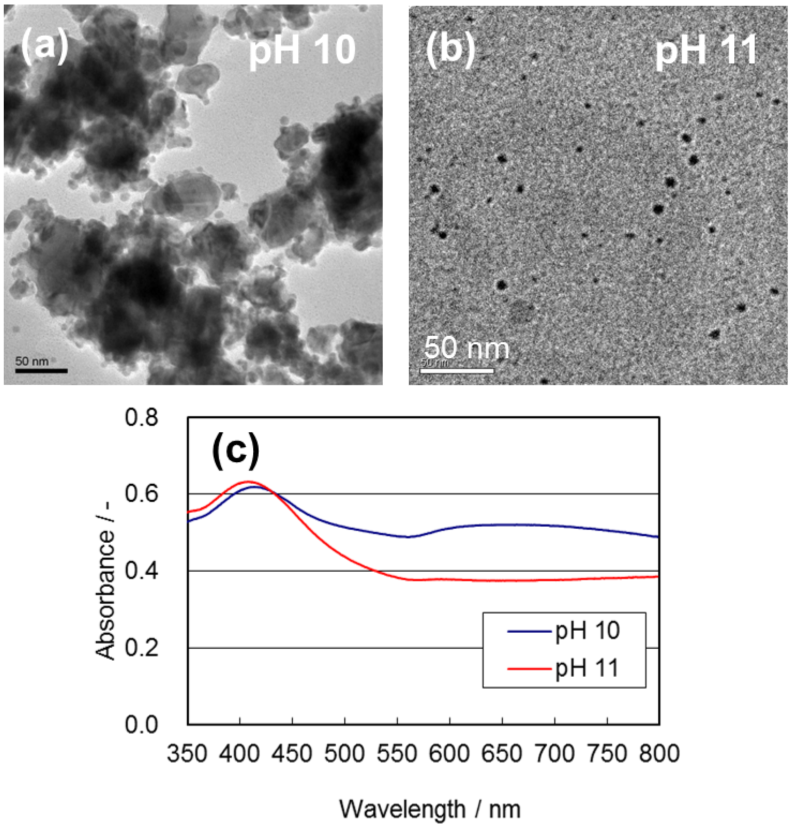

Fig. S8 TEM images of Cu@Ag nanoparticles synthesized at (a) pH 10, (b) pH 11 and the corresponding (c) UV-vis spectra of the nanoparticle dispersions. At pH 11 only Ag nanoparticles were formed.

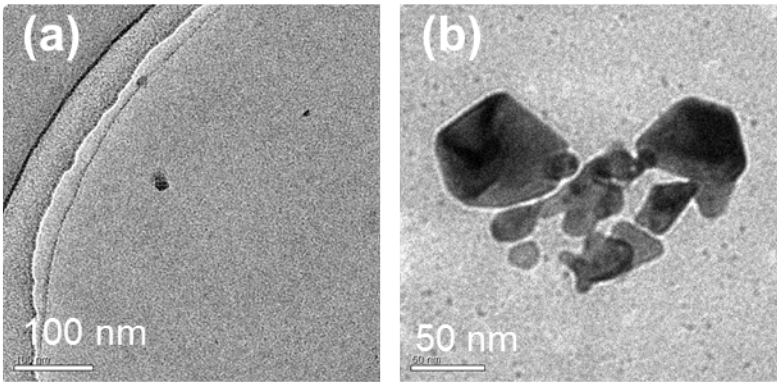

Fig. S9 TEM images of (a) Cu nanoparticles after stored 1 day in ethanol and (b) Cu@Ag core–shell nanoparticles after stored 7 days in ethanol. Only limited number of Cu nanoparticles (maximum size 15 nm) was found because most of Cu nanoparticles were dissolved by spontaneous oxidation. Despite the spherical nanoparticles turned to irregular shapes, Cu@Ag nanoparticles remained in the solution after 7 days, indicating the longer life of the core-shell structure.